SIMULTANEOUS RETRIEVAL OF AEROSOL AND SURFACE OPTICAL PROPERTIES USING MULTI-ANGLE IMAGING SPECTRORADIOMETER (MISR) DATA

J. Keller [a], *, S. Bojinski [b], A. S. H. Prevot [a]

[a] Paul Scherrer Institute, Laboratory of Atmospheric Chemistry (LAC),
5232 Villigen PSI, Switzerland - johannes.keller@psi.ch
[b] World Meteorological Organization (WMO), Global Climate Observing System Secretariat (GCOS),
1211 Geneva 2, Switzerland

KEY WORDS: Remote Sensing, Aerosols, Satellite, MISR, Retrieval Algorithm

ABSTRACT:

The operational aerosol product of the Multi-angle Imaging SpectroRadiometer (MISR) is available only for a grid cell size of 17.6 km. This spatial resolution is too coarse for studies in complex terrains like Switzerland. An algorithm for retrieving simultaneously aerosol and surface optical properties at a resolution of 1.1 km was developed. It uses MISR subregion radiance data of the 9 cameras and 4 spectral bands to generate characteristic functions $\rho_{surf} = f_{\lambda,cam} (\beta_e (550 \text{ nm}))$, where $\beta_e (550 \text{ nm})$ and ρ_{surf} are the ground level aerosol extinction coefficient at 550 nm and the surface reflectance, respectively. The analysis of the mutual intersections of those functions yield optimum values for $\beta_e (550 \text{ nm})$, aerosol optical depth (AOD) at 550 nm and ρ_{surf}. MODTRAN 4 v3r1 was used to create radiance look-up tables. The algorithm was tested for MISR paths covering Switzerland and northern Italy. Results of two days (low and high aerosol loads on May 14 and June 17, 2002, respectively) were analyzed and compared with sun photometer measurements. First, ground level aerosol extinction coefficients and optical depth over water were derived. From those data it was possible to retrieve a best-fit aerosol mixture. AOD (550 nm) over water are in satisfactory agreement with both sun photometer data and the operational aerosol product of MISR. Second, the Ross-Li approach for the bidirectional reflectance factor (BRF) supported by MODTRAN 4 was applied to simulate the radiance over vegetation surfaces. In this case the retrieved aerosol extinction coefficients and optical depths over vegetation are significantly lower than the values derived over water. We assume that the incomplete coupling of BRF and radiation in MODTRAN 4 is at least partly responsible for this discrepancy.

1. INTRODUCTION AND SCOPE

MISR aboard the Terra satellite observes the earth with 9 cameras (Df to Af: forward, An: nadir, Aa to Da: aftward) in 4 spectral bands (446, 557, 672 and 866 nm) (Figure 1). Numerous operational products are available, in particular geo-rectified radiance (275 and 1100 m resolution, depending on camera and spectral band), optical and microphysical properties of standard aerosol components and mixtures, best fit aerosol optical depth (AOD) and best fit aerosol mixture (Diner *et al.*, 1998; NASA/ASDC, 2002). The MISR aerosol product (17,6 km resolution), however, is too coarse for studies in complex domains such as Switzerland. A novel algorithm is capable of retrieving simultaneously ground level extinction coefficient, AOD, aerosol mixture and surface reflectance on a resolution of 1.1 km. Details are published in Keller *et al.*, 2007.
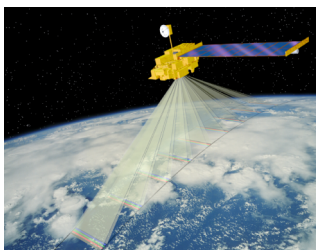

Figure 1: Multi-angle Imaging SpectroRadiometer (MISR)

2. SIMULTANEOUS RETRIEVAL (SR) ALGORITHM

Let us assume an idealized atmosphere with given trace gas and aerosol compositions and profiles located at northern mid-latitude. The widely used radiative transfer model (RTM) MODTRAN 4 (Berk *et al.*, 1999; Berk *et al.*, 2003) is designed to simulate the Top of Atmosphere (TOA) spectral radiance for given geometric, atmospheric and surface parameters, in particular the TOA radiance of the spectral band λ for the view geometry of each camera *cam*. The current release is v3r1. Input data may be explicitly specified, e.g. vertical profiles of meteorological parameters and atmospheric constituents, optical properties of aerosols). The basic optical quantity used as a variable input is the extinction coefficient $\beta_e (550 \text{ nm})$. Wavelength dependent extinction and absorption coefficients are specified relative to that value. MODTRAN 4 supports the DISORT N-stream option for multiple scattering in inhomogeneous atmospheres. Optical properties of the ground surface may be specified either as lambertian or by Bidirectional Reflectance Distribution Functions (BRDFs). In an inter-comparison workshop in the framework of ACCENT / TROPOSAT 2 (Wagner *et al.*, 2007) 10 RTMs based on different algorithms were tested for various geometries and vertical atmospheric profiles. Since the workshop was focused on Multi-Axes Differential Absorption Spectroscopy (MAXDOAS), only upward-looking view paths were included. The MODTRAN 4 radiances show a close match to the results of the other models. Hence, we are confident that MODTRAN 4

---

* Corresponding author.

correctly models scattering and absorption of radiation by gaseous and particulate constituents of the atmosphere. The tropospheric aerosol column density of a given vertical profile is varied by adjusting the aerosol extinction coefficient β_e (550 nm) at ground level.

In the simplest case the ground surface is a lambertian reflector with variable reflectance ρ_{surf}. Figure 2 shows a typical relationship of the simulated TOA apparent reflectance ρ_{app} (proportional to the TOA radiance) vs. the scattering angle of the camera Df to Da for β_e (550 nm) = 0.0 (thin solid), 0.2, 0.4 (dotted) and 0.6 km^{-1} (thick solid), and ρ_{surf} = 0.0 (left panel) and 0.2 (right panel). It is evident from Figure 2 that in the case of a substantial aerosol load the cameras looking forward at large zenith angles (e.g. Df) observe the same location as an apparently brighter target than the corresponding aftward looking sensors (e.g. Da). At low surface reflectance (e.g. ρ_{surf} = 0.0) enhanced aerosol loads brighten the target. For bright surfaces (not shown) the observed radiance decreases due to extinction of the reflected radiation.
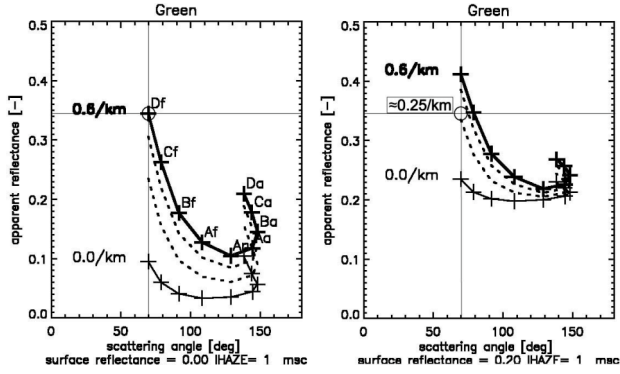

Figure 2: Simulated TOA apparent reflectance ρ_{app} of the 9 cameras over a lambertian target vs. scattering angle for the green spectral band. Ground level β_e(550 nm) is set to 0 (thin solid), 0.2, 0.4 (dotted, not labelled) and 0.6 km^{-1} (thick solid). ρ_{surf} is set to 0 (left) and 0.2 (right). For camera Df and ρ_{surf}=0.0, ρ_{app}=0.345 is obtained for β_e(550 nm)=0.6 km^{-1}. The same ρ_{app} results for ρ_{surf}=0.2 and β_e(550 nm)=0.25 km^{-1}.

For β_e (550 nm) = 0.6 km^{-1} and ρ_{surf} = 0.0 (left panel of Figure 1), the apparent reflectance observed by camera Df in the green band is about 0.345 (see crosshair). The simulation yields the same radiance, i.e. the same apparent reflectance, also for other data pairs [β_e (550 nm), ρ_{surf}], e.g. β_e (550 nm) ≈ 0.25 km^{-1} and ρ_{surf} = 0.2 (right panel). In other words, over dark targets a small increase of the surface reflectance must be compensated by decreased aerosol scattering to keep the apparent reflectance constant. Hence it is possible to generate characteristic functions $\rho_{surf} = f_{\lambda,cam}\left(\beta_e(550\,\text{nm})\right)$. These functions are derived from the camera and wavelength dependent radiance L (λ,cam) for specified reference values $\beta_{e,ref}$ $(550$ nm$)$ and $\rho_{surf,ref}$ (look-up tables, LUT). In Section 3 an example of those functions is given (Figure 4). If all atmospheric and surface properties correspond to reality, the characteristic functions of all cameras should intersect at one single point. Note that in theory the intersection values of β_e $(550$ nm$)$ are independent of λ, i.e. of the spectral band used for the calculation of the LUT, because β_e $(550$ nm$)$ controls the radiative transfer model.

In reality, we expect a clustering of the intersections with most probable values $\beta_{e,\lambda}(550\,\text{nm})$ for each spectral band λ. TOA

radiances simulated for the most likely aerosol mixture, for $\overline{\beta_e}\left(550\,\text{nm}\right)$ and for $\rho_{surf,\lambda}$ are supposed to agree best with the MISR radiances of all cameras and spectral bands. In this case the retrieved $\beta_{e,\lambda}(550\,\text{nm})$ of each spectral band λ are expected to scatter least around the best-fit average $\overline{\beta_e}\left(550\,\text{nm}\right)$. Finally, most likely vertical AODs are calculated using the best fit $\overline{\beta_e}\left(550\,\text{nm}\right)$ as input for the simulation. If we use the LUTs for an unrealistic aerosol mixture, the retrieved values of $\beta_{e,\lambda}(550\,\text{nm})$ depend significantly on the spectral band leading to a larger scatter.

3. RESULTS

The SR algorithm was applied to a region of interest that includes Switzerland and parts of the adjacent countries MISR data were analyzed for two overpasses on May 14 (low aerosol loads) and June 17, 2002 (high aerosol loads). Figure 3 shows the RGB MISR radiance image of the nadir looking camera An together with the water target and sun photometer locations used for the analysis.
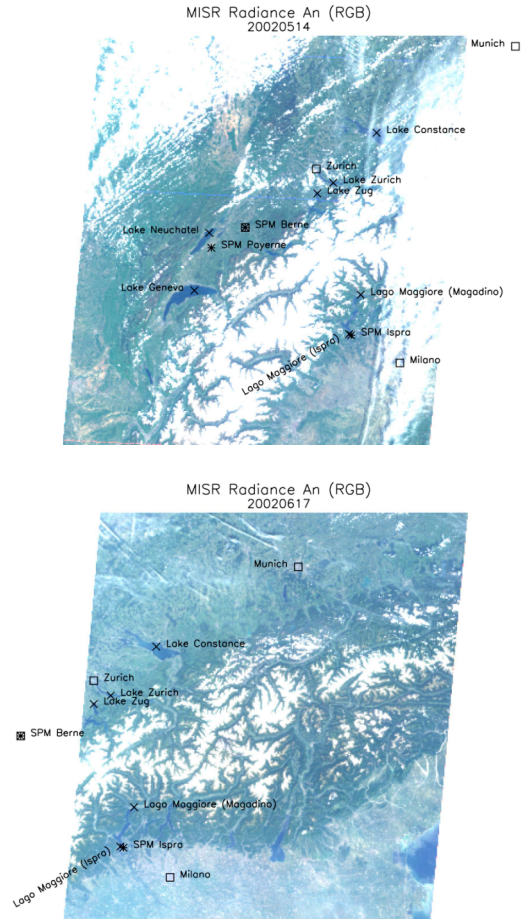

Figure 3: RGB MISR radiance image of the nadir looking camera An. x : water targets; * : sun photometer (land) targets. Top panel: May 14, 2002 (low aerosol loads), bottom panel: June 17, 2002 (high aerosol loads).

Radiance LUTs were calculated for 7 lake targets shown in Figure 3. A lambertian surface and selected aerosol mixtures of

the MISR aerosol product were specified for the MODTRAN 4 input. The characteristic functions $\rho_{surf} = f_{\lambda,cam}(\beta_e(550\,nm))$ for each camera and spectral band are depicted in Figure 4. In this example, MISR radiance data of a subregion over Lago Maggiore close to the sun photometer site Ispra was taken to derive those functions. The figure shows the functions for the best fit aerosol mixture 18, which is composed of 75% sulphate-like fine particles and 25% red dust (see Keller *et al.*, 2007 for details). It is evident that for these optimum conditions the intersections of the characteristic functions cluster very well, especially for the green and the red band. Moreover, the retrieved values $\overline{\beta}_{e,\lambda}(550\,nm)$ are nearly independent of the MISR spectral band. Finally, the vertical AOD for the assumed vertical atmospheric profile can be calculated from the transmittance LUT and from $\overline{\beta}_e(550\,nm)$. The SR algorithm is capable of retrieving distinct intersections only for clear and hazy conditions. If clouds are present, which have scattering properties different from those specified for aerosols in MODTRAN, the mutual intersections of the intersections do not cluster and no $\overline{\beta}_{e,\lambda}(550\,nm)$ can be retrieved. Hence clouds are automatically eliminated by this procedure.

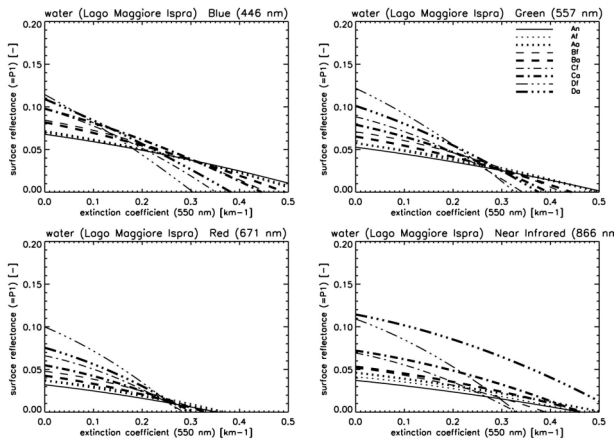Figure 4: Surface reflectance ρ_{surf} vs. ground level aerosol extinction coefficient $\beta_e(550\,nm)$ for the water target Lago Maggiore close to Ispra. The MISR radiances of the 4 MISR bands for June 17, 2002 and the look-up tables for the optimum mixture 18 were used to derive these functions. A lambertian surface reflectance was assumed.

Table 1 lists the most likely AOD at 550 nm and the associated aerosol mixture for the 7 lake targets taken from the SR algorithm results, from the MISR operational product and from close-by sun photometer measurements. For most water targets, the SR algorithm delivers similar aerosol optical depths and mixtures as the operational product. The Lago Maggiore data agree well with the AERONET sun photometer measurements at Ispra on May 14. For the greater AOD on June 17 the agreement is somewhat worse. Note that the MISR path does not cover Payerne and Bern on June 17.

Over vegetation the lambertian assumption for the surface reflectance is no longer valid. The angular dependence is described by the Bidirectional Reflectance Factor (BRF). There are various options in MODTRAN 4 v3r1 to select BRF models. In this study the Ross-Li approach (Lucht *et al.*, 2000) was chosen and radiance LUT for agriculture and forest were generated (see Keller *et al.*, 2007 for details). The analysis of the SR results for different vegetation and water targets and the

comparison with the MISR product and with the sun photometer at Ispra revealed that $\overline{\beta}_e(550\,nm)$ retrieved over vegetation is significantly less than the corresponding values over close-by Lago Maggiore. The difference is about 0.1 and 0.2 km^{-1} for May 14 (low aerosol concentrations) and June 17 (high aerosol concentrations), respectively. This leads to small AOD values retrieved for the sun photometer sites compared with the measurements and the MISR operational product. For low aerosol concentrations such as those at Payerne and Bern on May 14, the intersection values $\overline{\beta}_{e,\lambda}(550\,nm)$ are even negative.

After a careful analysis of the algorithm modules we came to the conclusion that the most likely source relevant for the inconsistencies is the radiation transfer model MODTRAN 4 v3r1. Because realistic AODs are retrieved over water, i.e. for dark, lambertian targets, and the MAXDOAS inter-comparison with other RTMs was successful we suppose that the discrepancies are due to an incomplete coupling of the non-lambertian surface and the radiation streams in the DISORT module of MODTRAN 4. According to information from the developer, the respective improvement announced already at the release of earlier versions is not yet implemented in v3r1. After a preliminary increase of $\overline{\beta}_e(550\,nm)$ over land by 0.1 and 0.2 km^{-1} for May 14 and June 17, respectively, AOD maps were drawn for both days (Figure 5). AOD values north of the Alps are generally lower than in the Po basin on both days. Increased aerosol loads are also found at the valley bottoms. Thin clouds and contrails, which appear as high aerosol concentrations, are detected on June 17 in the north of the scene as well. The algorithm automatically disregards thick clouds. The spatial features are similar to those of the MISR aerosol product (not shown).

4. CONCLUSIONS

A novel algorithm was developed, which is designed to retrieve simultaneously the near surface aerosol extinction coefficient, the aerosol optical depth, the aerosol mixture, and the surface reflectance. This simultaneous retrieval (SR) algorithm has the potential of providing realistic aerosol properties over lambertian water targets on a spatial resolution of 1.1 km., thus enhancing the resolution of the MIRS aerosol product (17.6 km). Aerosol optical depths over Lago Maggiore close to the sun photometer site Ispra agree well with measurements. For land targets, however, we found significantly lower aerosol extinction coefficients and optical depths than for close-by water. Differences of 0.1 km^{-1} and 0.2 km^{-1} for the green spectral band were estimated for May 14 and June 17, respectively. After an extended analysis of the results, including a RTM inter-comparison in the frame of the European network ACCENT, we believe that the full coupling of BRF and DISORT, which is not yet implemented in the current MODTRAN 4 version, is at least partly responsible for this disagreement. The scope of a new project is the confirmation of this conjecture, the improvement of the relevant modules in MODTRAN 4, and applications of the algorithm for an extended variety of atmospheric conditions and surface targets.

Date / Site	SR algorithm		MISR operational product		SPM
	AOD (550 nm)	Mix	*AOD* (557 nm)	Mix	*AOD* (550 nm)
May 14, 2002					
Lake Geneva	0.086±0.002	8	0.067±0.023	8	
Lake Neuchatel	0.082±0.004	5	0.056±0.013	8	
Lake Zug	0.243±0.022	18	n.a.	n.a.	
Lake Zurich	0.260±0.024	9	n.a.	n.a.	
Lake Constance	0.375±0.008	8	n.a.	n.a.	
Lago Maggiore (Magadino)	0.188±0.010	9	n.a.	n.a.	
Lago Maggiore (Ispra)	0.203±0.019	5	0.228±0.044	5	
SPM Payerne	n.a. [1]	n.a. [1]	0.076±0.024	10	0.02±0.001
SPM Bern	n.a. [1]	n.a. [1]	0.083±0.029	17	0.06±0.003
SPM Ispra	0.127±0.002	5	0.228±0.044	5	0.20±0.002
June 17, 2002					
Lake Geneva	n.a.	n.a.	n.a.	n.a.	
Lake Neuchatel	n.a	n.a.	n.a.	n.a.	
Lake Zug	0.320±0.010	18	n.a.	n.a.	
Lake Zurich	0.319±0.005	8	n.a.	n.a.	
Lake Constance	0.339±0.007	8	n.a.	n.a.	
Lago Maggiore (Magadino)	0.371±0.006	15	0.747±0.206	5	
Lago Maggiore (Ispra)	0.355±0.011	18	0.386±0.102	18	
SPM Payerne	n.a. [2]	n.a. [2]	n.a. [2]	n.a. [2]	0.33±0.020
SPM Bern	n.a. [2]	n.a. [2]	n.a. [2]	n.a. [2]	0.28±0.010
SPM Ispra	0.094±0.003	7	0.386±0.102	18	0.42±0.004

Table 1: Comparison of the best-fit AOD (550 nm) and mixture derived by the simultaneous retrieval (SR) method with the regional mean AOD and mixture of the MISR aerosol product, and with sun photometer AOD. The simultaneous retrieval algorithm assumes the BRF for agriculture when applied to the sun photometer sites.
[1] May 14, 2002: no SR AOD was calculated because of negative retrievals of the extinction coefficient.
[2] June 17, 2002: the MISR swath did not cover Lake Geneva, Lake Neuchatel, Berne and Payerne.
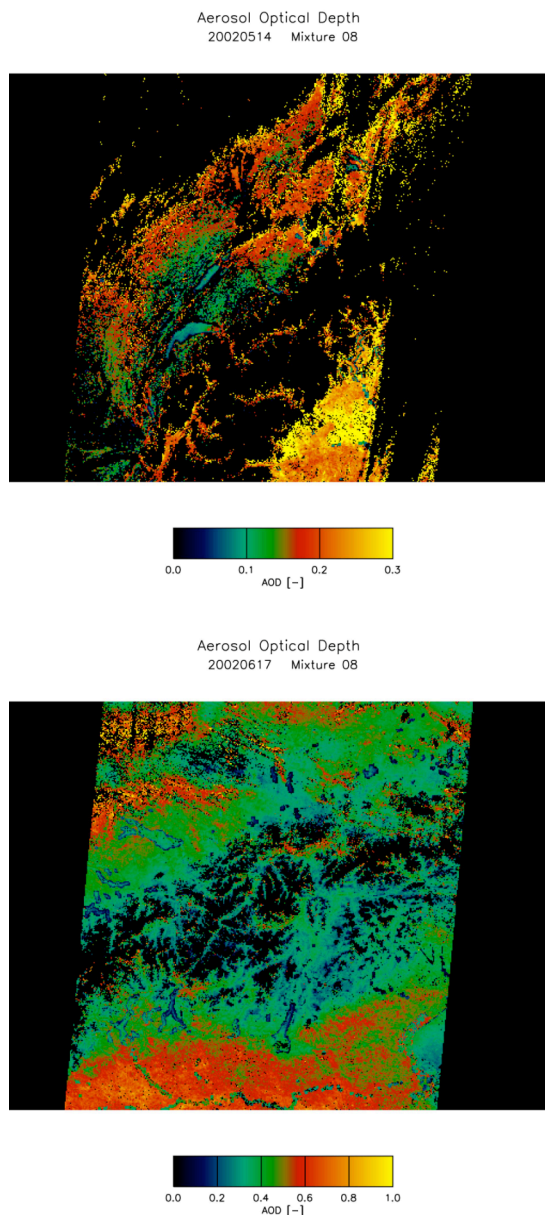

Figure 5: Aerosol optical depth AOD (550 nm) map derived with the simultaneous retrieval method for May 14 (low aerosol concentrations, top) and June 17, 2002 (high aerosol concentrations, bottom). Note the scale difference between those two days. See Figure 3 for related radiance maps.

5. REFERENCES

Berk A., Anderson G. P., Acharya P. K., Hoke M. L., Chetwynd J. H., Bernstein L. S., Shettle E. P., Matthew M. W., Adler-Golden S. M., 2003. *MODTRAN4 Version 3 Revision 1 User's Manual*. Air Force Research Laboratory, Space Vehicles Directorate, Air Force Materiel Command, Hanscom AFB, MA 01731-3010, Hanscom.

Berk A., Anderson G. P., Bernstein L. S., Acharya P. K., Dothe H., Matthew M. W., Adler-Golden S. M., Chetwynd J. H. J., Richtsmeier S. C., Pukall B., Allred C. L., Jeong L. S., Hoke M. L. a., 1999. MODTRAN4 Radiative Transfer Modelling for Atmospheric Correction. *SPIE Proceeding on Optical Spectroscopic Techniques and Instrumentation for Atmospheric and Space Research III* 3756, 348-353.

Diner D. J., Beckert J. C., Reilly T. H., Bruegge C. J., Conel J. E., Kahn R., Martonchik J. V., Ackerman T. P., Davies R., Gerstl S. A. W., Gordon H. R., Muller J.-P., Myneni R., Sellers R. J., Pinty B., Verstraete M. M., 1998. Multiangle Imaging SpectroRadiometer (MISR) description and experiment overview. *IEEE Transactions on Geoscience and Remote Sensing* 36, 4, 1072-1087.

Keller J., Bojinski S., Prevot A. S. H., 2007. Simultaneous retrieval of aerosol and surface optical properties using data of the Multi-angle Imaging SpectroRadiometer (MISR). *Remote Sensing of Environment* 107, 1-2, 120-137.

Lucht W., Schaaf C. B., Strahler A. H., 2000. An algorithm for the retrieval of albedo from space using semiempirical BRDF models. *IEEE Transactions on Geoscience and Remote Sensing* 38, 2, 977-998.

NASA/ASDC, 2002. MISR Data and Information. http://eosweb.larc.nasa.gov/PRODOCS/misr/data.html.

Wagner T., Burrows J., Deutschmann T., Dix B., Hendrick F., von Friedeburg C., Frieß U., Heue K.-P., Irie H., Iwabuchi H., Keller J., McLinden C., Oetjen H., Palazzi E., Petrotoli A., Platt U., Postylyakov O., Pukite J., Richter A., van Roozendael M., Rozanov A., Rozanov V., Sinreich R., Sanghavi S., Wittrock F., 2007. Comparison of box-air-mass-factors and radiances for MAX-DOAS-geometries calculated from different UV/visible radiative transfer models. *Atmospheric Chemistry and Physics* (in press).

6. ACKNOWLEDGEMENTS